

# **In Vivo Determination of the Complex Elastic Moduli of Cetacean Head Tissue**

Peter H. Rogers

G. W. Woodruff School of Mechanical Engineering

Georgia Institute of Technology

Atlanta, GA 30332

phone: (404) 894-3235 fax: (404) 894-7790 email: [peter.rogers@me.gatech.edu](mailto:peter.rogers@me.gatech.edu)

David H. Trivett

G. W. Woodruff School of Mechanical Engineering

Georgia Institute of Technology

Atlanta, GA 30332

phone: (404) 385-1870 fax: (404) 894-7790 email: [david.trivett@me.gatech.edu](mailto:david.trivett@me.gatech.edu)

Award Number: N00014-05-1-0658

## **LONG-TERM GOALS**

The overall goal of this project is to determine the feasibility of *in vivo*, non-invasive measurement of the complex elastic moduli of cetacean head tissue. If this objective is met, measurement systems could be developed capable of measuring the complex elastic moduli of the head tissue of live, stranded cetaceans.

## **OBJECTIVES**

The technical objective is to remotely generate and detect mid-frequency (1 to 10kHz) elastic waves within the body of a living cetacean, using ultrasound and to use the measured propagation parameters of these waves to obtain the complex elastic moduli by inversion. A further technical objective is to extract tissue moduli in this manner intracranially. This objective carries considerably more technical risk since both the wave-generating ultrasound and the probe ultrasound will be attenuated, distorted and scattered by the passage through the skull.

## **APPROACH**

The approach is to measure the complex shear and bulk modulus, from which all other moduli can be calculated. The shear modulus will be determined by measuring the speed and attenuation of shear waves generated within the tissue using focused ultrasound as a remote localized force generator. This general approach to determining the complex modulus is an application of a new medical imaging technology called elastography. The methods described by Greenleaf (Chen et al, 2002) and Sarvazyan (Sarvazyan et al, 1998) provide the basis for shear wave generation. Displacements are generated remotely in a tissue volume using one or more focused ultrasound beams. In the single-beam case, the ultrasonic carrier signal is modulated at a low frequency  $\Delta f$ . In the dual-beam confocal configuration, the two ultrasonic signal carrier frequencies are offset from each other by  $2\Delta f$ . In both cases, a radiation force at the focal point primarily generates shear waves at the frequency  $2\Delta f$ .

Report Documentation Page				Form Approved OMB No. 0704-0188	
Public reporting burden for the collection of information is estimated to average 1 hour per response, including the time for reviewing instructions, searching existing data sources, gathering and maintaining the data needed, and completing and reviewing the collection of information. Send comments regarding this burden estimate or any other aspect of this collection of information, including suggestions for reducing this burden, to Washington Headquarters Services, Directorate for Information Operations and Reports, 1215 Jefferson Davis Highway, Suite 1204, Arlington VA 22202-4302. Respondents should be aware that notwithstanding any other provision of law, no person shall be subject to a penalty for failing to comply with a collection of information if it does not display a currently valid OMB control number.					
1. REPORT DATE <b>2008</b>		2. REPORT TYPE		3. DATES COVERED <b>00-00-2008 to 00-00-2008</b>	
4. TITLE AND SUBTITLE <b>In Vivo Determination of the Complex Elastic Moduli of Cetacean Head Tissue</b>				5a. CONTRACT NUMBER	
				5b. GRANT NUMBER	
				5c. PROGRAM ELEMENT NUMBER	
6. AUTHOR(S)				5d. PROJECT NUMBER	
				5e. TASK NUMBER	
				5f. WORK UNIT NUMBER	
7. PERFORMING ORGANIZATION NAME(S) AND ADDRESS(ES) <b>Georgia Institute of Technology, G. W. Woodruff School of Mechanical Engineering, Atlanta, GA, 30332</b>				8. PERFORMING ORGANIZATION REPORT NUMBER	
9. SPONSORING/MONITORING AGENCY NAME(S) AND ADDRESS(ES)				10. SPONSOR/MONITOR'S ACRONYM(S)	
				11. SPONSOR/MONITOR'S REPORT NUMBER(S)	
12. DISTRIBUTION/AVAILABILITY STATEMENT <b>Approved for public release; distribution unlimited</b>					
13. SUPPLEMENTARY NOTES					
14. ABSTRACT					
15. SUBJECT TERMS					
16. SECURITY CLASSIFICATION OF:			17. LIMITATION OF ABSTRACT <b>Same as Report (SAR)</b>	18. NUMBER OF PAGES <b>8</b>	19a. NAME OF RESPONSIBLE PERSON
a. REPORT <b>unclassified</b>	b. ABSTRACT <b>unclassified</b>	c. THIS PAGE <b>unclassified</b>			

The particle displacements resulting from the passage of the propagating shear wave can be detected remotely using a modified version of an ultrasonic Doppler vibration measurement system called NIVAMS developed at Georgia Tech (see Cox and Rogers, 1987, Martin et al, 2002). The system will be modified to make the transmitting and receiving beams coaxial in order to permit operation in tight quarters. Algorithms will be developed to enable the magnitude and phase of vibration to be determined, as well as the range at which the vibration is being measured. By measuring the amplitude and arrival time of the shear wave at two different points the propagation speed and attenuation can be determined.

Elastic waves will be both remotely and directly generated in tissue phantoms and measured both remotely and directly to validate the measurement technique. The elastic properties of tissue phantoms will be obtained from remotely generated and measured data and compared with directly measured and tabulated material values. The noninvasive technique will be repeated for tissue phantoms enclosed in a simulated or hydrated real cetacean skull, and with harvested tissue samples. Ultimately, feasibility will be assessed through measurements on a Navy bottlenose dolphin. The animal tests will be done initially for accessible tissue and subsequently for intracranial tissue. Ultrasound intensity and exposure time will be consistent with limits that have been established as safe for humans and frequencies will be kept high enough to be far above the highest frequency that is audible to the animal. The measurements should be harmless and painless.

## **WORK COMPLETED**

**1. Ultrasonic Vibrometer Development** A prototype range-resolving ultrasonic vibrometer was developed and its performance was demonstrated through a series of tests with a tissue phantom which mimics the ultrasonic properties of mammalian brain. The system concept was validated through the observation of shear wave displacements and calculation of their propagation speed from measurements of delay as a function of position.

**2. System Characterization** The behavior of the combined ultrasonic force generation and vibration measurement systems was examined in the laboratory using a suspended point scatterer. This was particularly useful for characterizing the force generation system in terms of drive level and effective beamwidth.

## **RESULTS**

### **1. Ultrasonic Vibrometer Development**

In previous work, two different techniques have been used for ultrasonic vibrometry. The first of these involved a pure tone ultrasonic carrier signal from which a phase modulation produced by the displacement of a reflecting surface was extracted to compute the time history of the surface displacement. This technique permitted the transduction of very small displacements (amplitudes on the order of a millionth of the ultrasonic wavelength) but did not allow for differentiation between individual scatterers contributing to the received signal. Thus it would not have permitted the interrogation of a weak scatterer such as cetacean brain tissue directly behind a strong scatterer such as bone. The second technique involved a pulsed ultrasonic carrier signal from which the motion of a reflecting surface was extracted by repeated correlation of the echoed pulses with those that were transmitted. This technique permitted different scatterers to be simultaneously interrogated, but required that the motion of the scatterers be relatively large (amplitudes great than a tenth of a wavelength). Shear motions of this size cannot be practically or safely generated in vivo. The

technique that is currently being developed is intended to combine the measurement resolution of pure-tone vibrometry with the spatial resolution of pulse-echo vibrometry.

The new technique requires that the ultrasonic carrier be a continuous signal made up of a large number of discrete tones that have a high spectral purity (less than -100 dB spectral side-lobes at greater than 2 Hz separation from each tone). This allows for the received signal to be decomposed into two components with different time dependences by using a novel spectral interpolation and pulse compression technique. One of these components (the carrier) is dependent only on the high-frequency time scale of the ultrasonic signal, and the other (the modulation) is dependent only on the low-frequency time scale of the acoustic path length modulation. The two components can be separated in the frequency domain and then be recombined to give a displacement history of all the scatterers contributing to the received signal as a function of the mean acoustic path length to each. With appropriate hardware and signal post-processing, this technique yields displacement resolution comparable to pure-tone vibrometry at the center frequency of the carrier signal and spatial resolution superior to pulsed vibrometry exploiting a comparable overall bandwidth. This improvement in spatial resolution is achieved by combined the results of two pulse compressions, which make use of compression waveforms that are in quadrature with each other. The functional representation of this combination is as follows:

$$\delta_m(t)_{tl} = \frac{I_{\text{mod}} \Big|_t \frac{dI_{\text{car}}}{dt} \Big|_{th} + Q_{\text{mod}} \Big|_t \frac{dQ_{\text{car}}}{dt} \Big|_{th}}{\frac{2}{c_h} \left( \left( \frac{dI_{\text{car}}}{dt} \right)_{th}^2 + \left( \frac{dQ_{\text{car}}}{dt} \right)_{th}^2 \right)} \quad [1]$$

Where  $\delta_m(t)_{tl}$  is the displacement of the  $m^{\text{th}}$  scatterer, the  $I$  and  $Q$  values represent the result of the two pulse compressions, the *car* and *mod* subscripts indicate the separated carrier and modulation terms respectively, and  $c_h$  is the propagation speed of the ultrasonic signal. The relationship is valid for  $t_h$  corresponding to the two-way propagation time to the  $m^{\text{th}}$  scatterer. Implementation of equation 1 gives a complete time history of the displacement in pseudo real time (processing time is currently about ten times data acquisition time on a desk top PC, but this is limited primarily by memory access speed).

As implemented, the prototype system exploited a carrier signal with 101 discrete tones separated by 6.25 kHz and centered on 2.5 MHz. This sampled low-frequency vibration in the range of 2 Hz to 3.12 kHz at 960 points within a brain-mimicking tissue phantom (Blue Phantom Inc.). The measurement points spanned from the face of concentric transmitting and receiving transducers to a depth of 11.5 cm inside the phantom. The measurement depth, measurement resolution, and the ability to separately depict motion at each individual point depend on a variety of factors related to properties of both the tissue and the transmit signal. Attenuation must be both sufficiently small to permit measurements to the full depth possible with the tonal spacing of the transmitted signal and sufficiently large to preclude spatial ambiguities caused by wrap around phenomena in the integral transforms used in the pulse compressions. This in turn dictates the center frequency of the ultrasonic carrier signal as attenuation is highly frequency dependent. The ability to separate points in space depends on homogeneity (speckle scatter) of the tissue and on the bandwidth of the carrier. In general, an increased bandwidth improves the spatial resolution by permitting compression pulses with shorter duration. In practice, this bandwidth is limited by hardware. It is difficult to distinguish the motion of a region of weak scattering

in close proximity to a region of strong scattering in much the same way that these regions are shadowed in conventional pulse-echo ultrasonic imaging.

Initial testing of the ultrasonic vibrometer involved direct mechanical excitation of shear waves in a tissue phantom suspended in a water filled tank, as shown in Figure 1. This was done in order to simplify the experimental system and facilitate refinement of the hardware and processing algorithms. In this configuration, the phantom was driven on one side by a 19mm polycarbonate sphere that was compelled to an electrodynamic shaker by means of a narrow stinger. The motion of the sphere was along an axis at a shallow angle to the surface of contact. This excited an outwardly propagating spherical shear wave in the phantom with an amplitude that was relatively constant over a large volume and could be controlled to match the amplitudes expected from radiation force excitation. The vibrometer was implemented with a dual-ring confocal ultrasonic transducer, with one ring radiating the carrier signal and the other ring receiving the backscattered pressure.

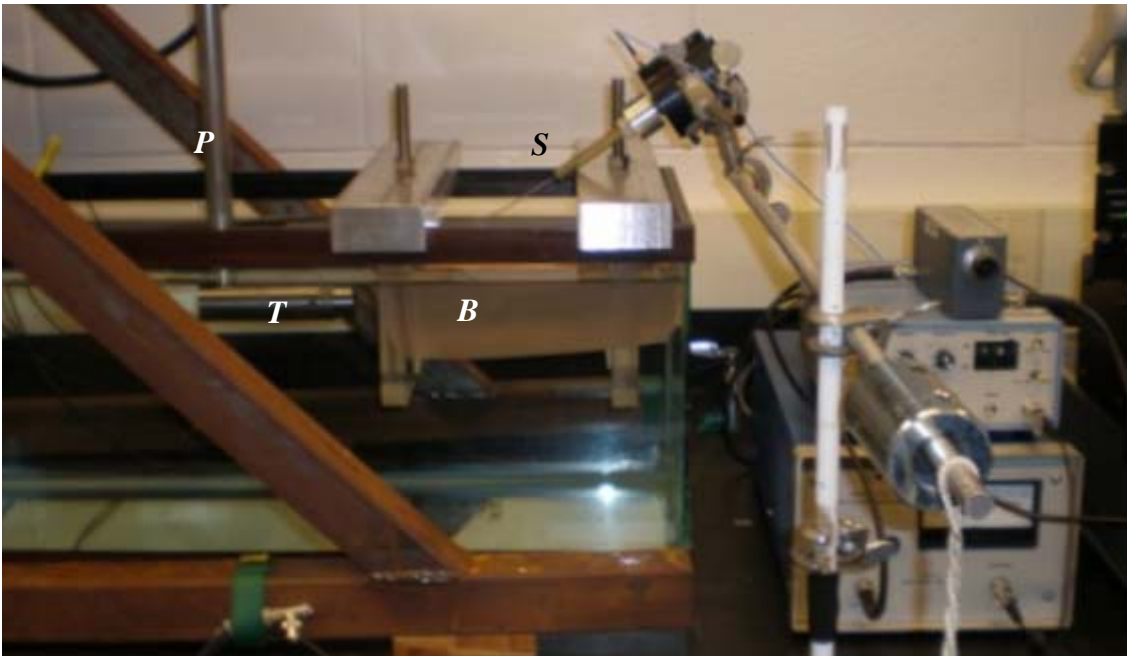


**Figure 1. Vibrometer test setup. Shear waves were generated by an external vibration source (S). The vibrometer transducer (T) was attached to a positioner (P) to facilitate scanning. The phantom (B) and transducer were submerged in a water tank.**

Figure 2 shows the displacements from one of these measurements at all 960 points plotted in groups of 120 on a  $\pm 4\mu\text{m}$  scale. Here the shear excitation signal was a swept-frequency chirp and the data was analyzed in a band from 2 Hz to 200 Hz. Close to the ultrasonic transducers (upper left of the figure) the measurement is overwhelmed by noise. This region is in the water outside the tissue phantom. The high noise floor here is a consequence of weak scattering from the water. Mathematically, this corresponds to a null in the denominator of equation 1. Over the remainder of the beam the measured time waveform clearly corresponds to the excitation signal. The interference midway through the waveform is attributable to the shear wave reflection from the bottom surface of the phantom. At long ranges the signal-to-noise ratio diminishes due primarily to a rising noise floor rather than a falling signal level. This is because the attenuation in the phantom reduces the energy returned in the ultrasonic carrier at longer ranges.

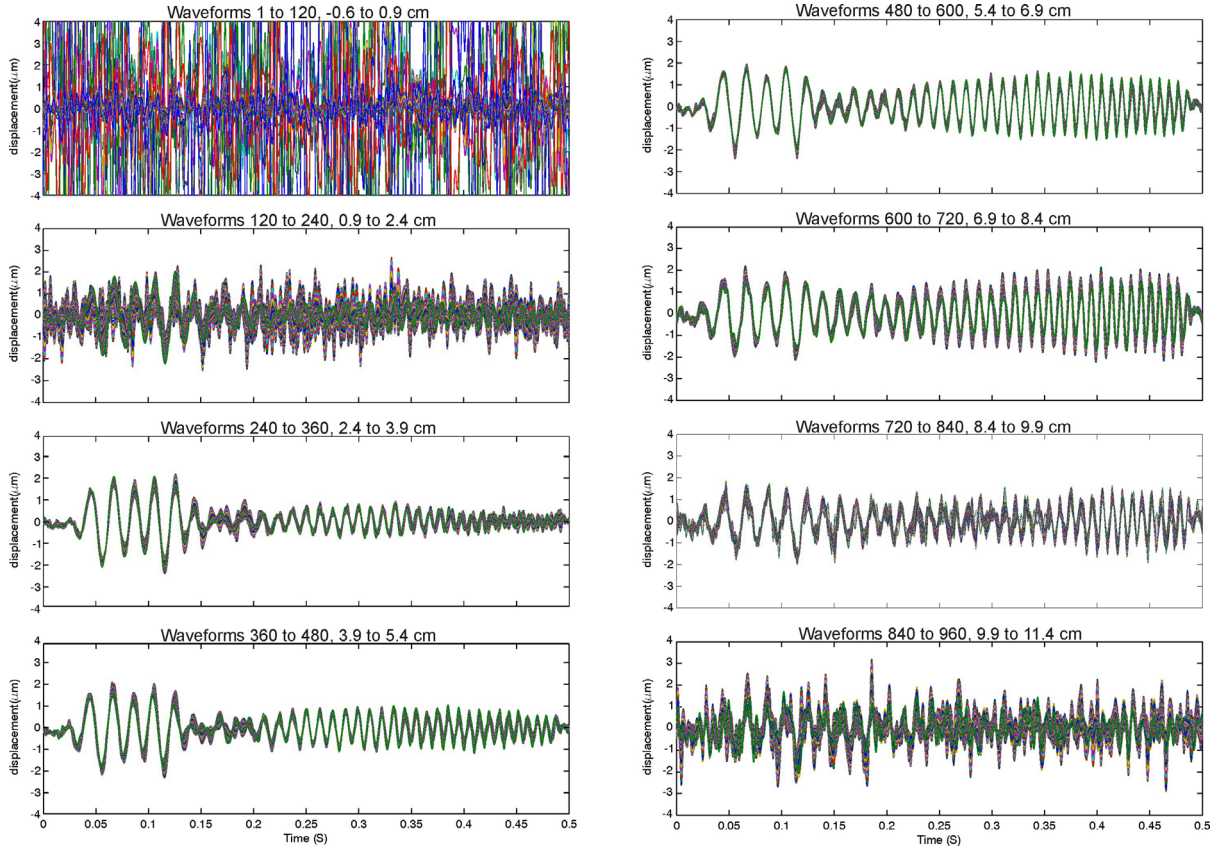


**Figure 2: Measured displacement time histories at 960 locations along an ultrasonic interrogation beam inside a tissue phantom. Signals shown in the upper left plot are in the water path between the transducers and the phantom. Signals shown in the lower right plot are furthest into the phantom and indicate increased noise due to attenuation of the ultrasonic carrier.**

In Figure 3 the delay times resulting from a cross correlation of each measured displacement time waveform with the shaker drive signal are plotted for all of the locations along the beam. Here, the ultrasonic transducers were located three different distances away from the spherical shear-wave source. Also depicted on this figure is the expected delay over these locations that was computed from a separate resonant-bar measurement of the bar wave speed characterizing the tissue phantom material. The measured data from the ultrasonic vibrometer can be seen the match this prediction quite well. The observed curvature of the delay measured along each beam individually also corresponds well to the distances from the source to each measured point. This is because the wavefronts were spherical and the beam linearly transected these.

In summary, the technique, hardware, and processing algorithms for a high precision depth-discriminating ultrasonic vibrometer have been developed and tested. The prototype system is capable of distinguishing the motion of regions a few millimeters apart and characterizing that motion to a precision of approximately  $1 \text{ nm}/\sqrt{\text{Hz}}$  with a 2.5 MHz center-frequency carrier signal. The practical limitations of this system are well understood and it appears to be suitable to the in vivo interrogation of a cetacean brain.

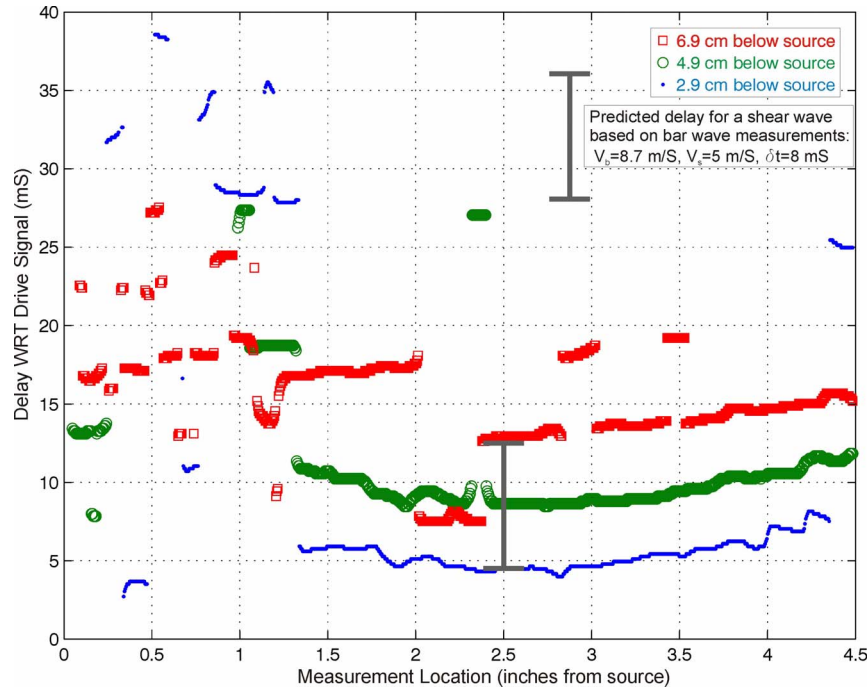


**Figure 3: Delay times as a function of depth in the ultrasonic interrogation beam for three transducer locations. The measured propagation delay is in good agreement with the expected value. Measurement locations less than approximately 1.0 inch from the transducer are in the water path between the transducer and phantom.**

## 2. System Characterization

The combined radiation force generation and vibrometer systems were characterized using the laboratory setup shown in Figure 4. The inner transducer was used as the vibrometer, and the outer transducer was used as the radiation force generator. A point scattering target was provided by suspending a 0.020" diameter stainless steel ball on a synthetic filament. Each transducer was fixed to a positioner to allow alignment and subsequent field scanning by translation of one transducer relative to the other. This is the general approach for the in vivo feasibility assessment prototype system<sup>1</sup>.

The test setup was used to check a variety of parameters, including force field shape as a function of drive configuration (amplitude modulated uniform drive vs dual ring offset carrier), "linearity" of induced displacement relative to the square of drive voltage, minimum detectable displacement, and measurement repeatability. Figure 5 shows the measured displacement of target as the forcing transducer, operated in the amplitude modulation configuration, is translated laterally away from the center of focus. The displacement ("direct") is normalized to the peak value and plotted along with the expected beam pattern ("calibration") based on a separate measurement of the radiated power from the transducer. The main lobe half-width of approximately 1mm is as expected. The observed displacement sidelobes are approximately 25% higher than predicted, although this is not expected to materially impact system performance. The data collected in the characterization runs showed the ability to remotely vibrate targets and measure the resulting displacements with an all-ultrasonic system, providing a basis for combined system testing with tissue phantoms now underway.

<sup>1</sup> For testing on tissue samples and marine mammals, a compact, lightweight positioner has been designed and built so that the device could be hand-held.

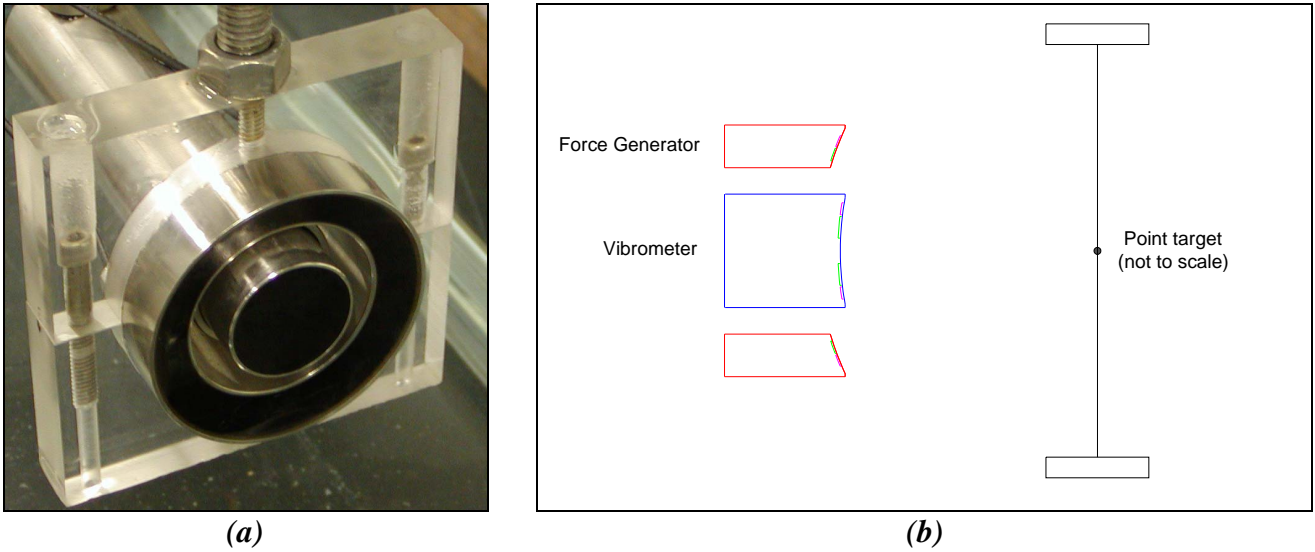


**Figure 4. System characterization test setup. (a) nested transducer configuration, (b) cross-section illustration with transducers focused on a point target**

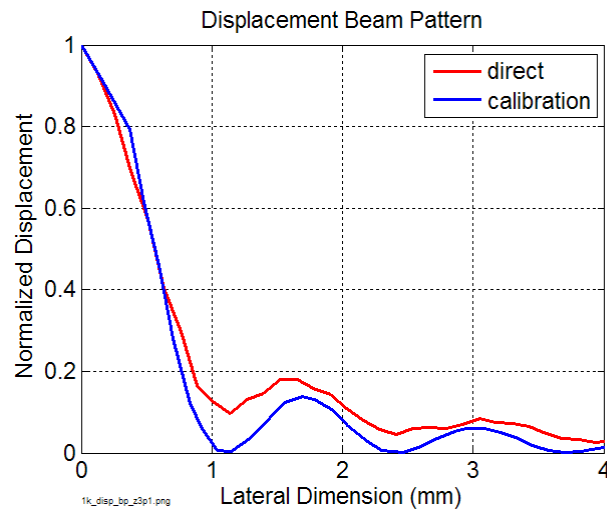


**Figure 5. Radiation force-induced displacement beam patterns. “Direct” refers to the result obtained with the ultrasonic force generation and reception systems. “Calibration” refers to a prediction based on a separate measurement of the forcing transducer’s radiated pressure field..**

## **IMPACT/APPLICATIONS** (Potential future impact for Science and/or Systems Applications)

There is considerable interest in the development of structural acoustic models for the cetacean head for two main reasons: 1) to better understand biomechanics of sound reception and production in cetaceans, and 2) to understand and hopefully mitigate any harmful effects of man-made sound on their health and behavior. The development and validity of these models is severely limited by an almost complete lack of knowledge of the mechanical properties of the constituent tissue. It is known that these properties change upon the death of the animal. There is thus considerable interest in being able

to measure these properties *in vivo*. The techniques and instrumentation investigated here should also have biomedical diagnostic application, including non-invasive examinations of stranded animals.

## **RELATED PROJECTS**

None

## **REFERENCES**

Chen S., Fatemi M., and Greenleaf J.F., “Remote measurement of material properties from radiation force induced vibration of an embedded sphere,” J. Acoust. Soc. Am., **112** , 884 (2002).

Cox, M. and Rogers, P.H., “Automated Noninvasive Motion Measurement of Auditory Organs in Fish Using Ultrasound”, J. of Vibration, Acoustics, Stress, and Reliability in Design, **109**, 55-59. (1987)

Finneran, J and Hastings, M., “A continuous-wave ultrasound system for displacement amplitude and phase measurement”, J. Acoust. Soc. Am, **115** , 3202-9, (2004)

Martin J.S., Fenneman et al., “Ultrasonic Displacement Sensor for the Seismic Detection of Buried Land Mines”. Proceedings of the SPIE: 2002 Annual International Symposium on Aerospace/Defense Sensing, Simulation, and Controls, Orlando, FL, **4742**, 606-616, (2002).

Martin, J.S. et al, “Ultrasonic vibrometer for seismic landmine detection”, Proc of the 18<sup>th</sup> International Congress on Acoustics, (2004)

Sarvazyan A, et al, “Shear Wave Elasticity Imaging: a new ultrasonic technology of medical diagnostics”, Ultrasound Med. Biol. 24(9), 1419-1435 (1998)

## **PUBLICATIONS**

Martin, J.S., Rogers, P.H., and Gray, M.D., “Ultrasonic vibrometer for tissue characterization”, 155th Meeting of the Acoustical Society of America, Paris, France (2008)

Gray, M.D., Martin, J.S., and Rogers, P.H., “Dual confocal ultrasound system for shear wave elastography”, 155th Meeting of the Acoustical Society of America, Paris, France (2008)